Design and Optimization of a Wing Structure for a UAS CLASS I 145 kg

João Jorge Miguel da Silva
jjsilva@academiafa.edu.pt

Academia da Força Aérea, Sintra, Portugal
June 2017

Abstract

In the context of air power in a Global scale, unmanned aerial systems (UAS) arise as one of the most promising developments of the last years. The Portuguese Air Force (FAP) has been developing UAS since 2008 which, although having been developed for R&D purposes, have already seen operational use, achieving significant results both nationally and internationally. These results have motivated the intent of using these platforms as part of the Portuguese weapons convoy that ensures surveillance missions over the vast area under Portugal's jurisdiction.The intent to use unmanned aerial systems in operational contexts demands for a significant increase of their design assurance level and reliability. In fact, as the safety of the over flown people must be ensured at all times, the use of such platforms must not only be able to adequately respond to demanding operational requirements, but also, comply with airworthiness requirements.

This work contributes to that intent by designing and optimizing the structure of the wing of a UAS with a maximum take-off weight of 145 kg (CLASS I), to be used for surveillance purposes. The work involved determining the loads acting on the structure, planning its general shape and components layout, choosing materials (composites), and then, shaping, sizing and optimizing it, for weight, strength and stiffness. In the optimization process, consideration was given to material cost and also to manufacture complexity. 3D geometric models were produced and structural numerical analyses were performed using finite element analysis - FEA. The optimization process used was based on a "chain top-down approach", which although simple, proved to be robust and effective. In order to account for the variability of the composite material properties introduced by the production techniques used, the material properties used in the FEA were determined experimentally by manufacturing and testing production samples. The resultant structure complied with every structural, weight and operational requirement, and showed to be simple and easy to build at an affordable manufacturing cost.
Keywords: Air power, FAP, UAS CLASS I, wing structural design, structural optimization, composites.

1. Introduction

Portugal has search and rescue (SAR) responsibilities over almost 6 million km^2 (square kilometers) of airspace from which 98% are over water (including interior waters, territorial sea and the Economic Exclusive Zone (EEZ)) [1] [2] [3] [4] [5], which makes Portugal the country holding the vastest water jurisdiction area in the European Union (EU), and the second vastest in the world [1] [2] [3] [6] [7] [8]. All of this areas require aerial presence either in the form of surveillance or patrol to ensure that the country's rights and duties are enforced and no illegal activities are performed. Also, monitoring is crucial to ensure border control and, therefore, the security and sovereignty of the Nation [4]. The size, importance and mandatory nature of these missions, requires the existence of means/equipment/platforms (aerial, maritime and ground), that can act in an integrated manner.

The Portuguese Air Force (FAP) has been developing UASs since 2008 under a project of Research, Development and Innovation (RD&I) called PITVANT (Project of Technological Investigation in Unmanned Aerial Vehicles) which have seen successful operational use, both nationally and internationally. However, service life of those platforms is ending due to limitations of its operational use and also due to the lack of a solid structural design which makes those platforms unsuitable for certification.

Due to the need for a new platform capable of fulfilling all the operational and airworthiness requisites of Search and Surveillance missions over the vast area under Portugal's jurisdiction, the present work aims to answer that need by designing and optimizing the structure of the wing of a new operational UAS, being developed, with a maximum take-off weight of 145 kg (CLASS I).

The design project had to fulfill the following structural, mass and operational requirements: Symmetric positive limit maneuvering load factor ≥ 3.8 and symmetric negative limit maneuvering load factor ≤ -1.5; high wing stiffness - wing tip displacement $\leq$

5% of the wing's half span; wing mass ≤ 26.2 [kg]; each half-wing capable of carrying an external suspended payload up to 10 [kg]; wing structure capable of being certifiable in terms of airworthiness.

The structural optimization process was conducted towards weight minimization and reduction of manufacturing costs.

The following conditions / restrictions were imposed to the project: wing's external geometry established by the UAVision preliminary designs; use the materials available at the FAP; wing had to allow for the internal routing of electric cables for the various electronic equipment and for the wing-tip lights; wing had to allow for the installation of "servo-motors" to control the ailerons and flaps; wing had to allow for the installation of wing-tips / winglets.

The totality of the work involved determining the loads acting on the structure (definition of the aircraft's flight envelope and identification of the wing's critical loading condition), planning the general shape and components layout, choosing materials (composites – manufacturing of specimens and experimental testing to obtain their properties), and then, shaping, sizing and optimizing its many components to give every part just enough strength without excess weight and also to reduce costs.

2. Implementation

2.1. Geometric Parameters Definition

The first step towards the wing's structural design consisted in obtaining a 3D model which was accomplished by using the modeling capabilities of the software *SolidWorks 2016 x64 Edition* (SW), the geometric information provided by the UAVision's preliminary design document [9] and additional airfoil geometric data from [10]. It allowed to better understand the wing's geometry, at to establish the structure's outer limits. See Figure 1.

When modeling the wing's surfaces, 3 [mm] gaps were created in-between the control surfaces (Flap and Aileron) and, between them and the main wing surface, to allow for their relative movement. Also, a specifically dimensioned gap was left between the main wing bottom surface and bottom leading edge surfaces of both the Flap and Aileron, to allow for their maximum deflections.

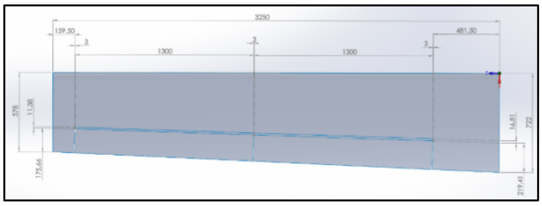

a)

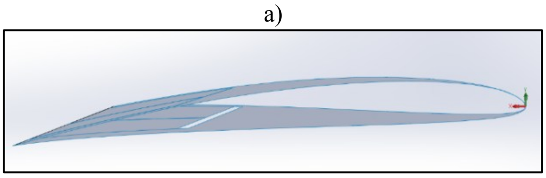

b)

Figure 1 - Wing's surface geometry (2D shells): a) Half-wing top view; Half-wing side view (root).

2.2. Forces Acting on the Wing

2.2.1. Combined Flight Envelope

The next step towards the structural design consisted in determining the aircraft's Flight Envelope which is a graph (diagram) that maps the possible combinations of maximum and minimum values of Speed (Equivalent Airspeed (EAS), V_e) vs Load Factor $\left(n = \frac{L}{W}\right)$ that an aircraft can experience during flight. Within this "envelope" the aircraft can operate without suffering any structural damage. This envelope results from the superposition of the *maneuvering envelope* (V-n diagram) and the *gust envelope* (V-g diagram). See Figure 2.

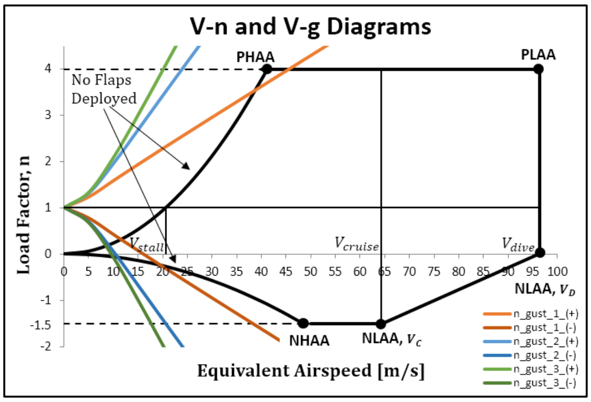

Figure 2 – Superposition of V-n and V-g diagrams.

Both the V-n and V-g were obtained for *sea level conditions* since aerodynamic forces typically have their maximum magnitudes when the aircraft is maneuvering at low altitude [11].

Because of the small mass of the aircraft (Maximum Take-off Weight (MTOW) of 145 Kg), the standard gust values of 25, 50 and 66 [ft. /s] or 7.62, 15.24, 20.12 [m/s] result in large values of load factor that greatly surpass the maneuver envelope and, therefore, don't allow for a typical combination of both diagrams. The solution was to discard the influence of the wing gusts (V-g) and consider that the flight envelope of the aircraft corresponds to the maneuvering envelope (V-n), only.

2.2.2. Wing Critical Loading Condition

Because the design of an aircraft structure is based on the largest expected load that it can endure, the Flight Envelope (V-n) was used to determine the wing's critical loading condition (during flight). That condition was identified as corresponding to the Positive Low Angle of Attack (PLAA) point, which corresponds to a situation in which the aircraft is performing a symmetric maneuver at maximum design / dive speed ($V_D \rightarrow V_e = 96.42\ [m/s]$) and reaching its limit load factor, $n_{limit} = 4$. See Figure 2 and 3.

For this aircraft, considering its main mission type (surveillance – far from acrobatic), the most probable flight maneuver and attitude, correspondent to that situation, was identified as being a "dive" followed by a "pull-up" maneuver and with the aircraft on a horizontal trajectory. See Figure 4.

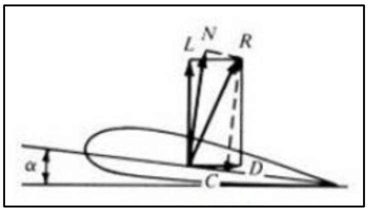

Figure 3 - Aerodynamic Force Resultants on an airfoil for the Positive Low Angle of Attack (PLAA) condition. Forces applied at the airfoil's *center of pressure* (C or CP) [12].

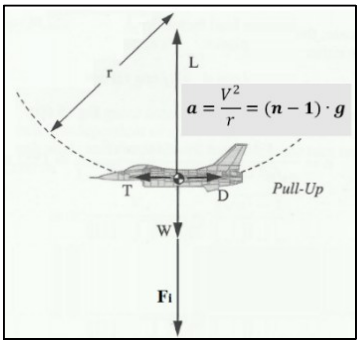

Figure 4 – "Pull-up" maneuver. Equivalent set of Static Conditions for the Accelerated Motion that is the maneuver. Forces acting on the aircraft's center of gravity: Lift (L); Weight (W); Inertial Force (Fi); Thrust (T); Drag (D); radius (r); velocity (V); acceleration (a); load factor (n); Earth's gravity acceleration (g).

According to the certification specifications [13], when designing an aircraft structure, the effect of the force resultant acting on the structure in each direction, should be studied separately.

Therefore, considering the objective of this work, the wing structure was designed to withstand the critical force resultant in the critical direction and no other forces resultants were considered simultaneously. The critical loading direction was identified as being the one perpendicular to the wing (y direction - wing coordinate system, see Figure 1). In that direction, the critical forces acting on the wing – in a static condition – were Lift, the wing's Weight and the wing's Inertial forces and the root forces resultant from the wing-to-fuselage attachment. The critical force resultant was given by:

$$\Sigma F_{perpendicular_{half-wing}} \approx \frac{L_{wing}}{2} - (\mathrm{W}_{half-wing} + F_{inertial})\cdot cos(\alpha)\cdot cos(\Gamma) + F_{root-cantilever} \quad (1)$$

Where α is the wing angle of attack and Γ is the wing's positive Deidre angle.

Further discretization and description of these forces and of their distributions, placement and associated moments was needed before any structural simulation could be run.

Lift

Using the SCHRENK's method a conservative estimation for the lift distribution along the wing span (z direction) was obtained, see Figure 5:

$$\bar{L}_{half\_wing}(z) = \frac{1}{2}\cdot\left[\frac{2\cdot L_{wing}}{b\cdot(1+\lambda)}\cdot\left[1-\frac{2\cdot z}{b}\cdot(1-\lambda)\right]+\frac{4\cdot L_{wing}}{\pi\cdot b}\sqrt{1-\left(\frac{2\cdot z}{b}\right)^2}\right], \text{ with } 0\le z\le b/2 \quad (2)$$

Where b is the length of the wing span, λ is the wing tapper ratio and,

$$L_{wing} \approx n_{design}\cdot W_{aircraft} = n_{design}\cdot MTOW\cdot g \quad (3)$$

Where g is the Earth's gravity acceleration for sea level conditions and,

$$n_{design} = SF_{loads}\cdot n_{limit} = SF_{loads\_standard}\cdot SF_{loads\_composites}\cdot n_{limit} \quad (4)$$

Where the SF_{loads} is the *load safety factor* which, in this case, is comprised by: $SF_{loads\_standard} = 1.5$ (≥1.5 is the standard for the aircraft industry for structures whose failure would lead to a Hazardous or more serious failure condition [14]), and by the $SF_{loads\_standard} = 1.5$ (≥1.5 applied for composite structures where specimen were tested with no specific allowance for moisture and temperature [14]).

The total lift value was equally obtained either from the integration of (2) or the division of (3) by 2.

Figure 5 – Lift distribution for half-wing.

Lift forces acting on the center of pressure (CP) are usually replaced by lift at the aerodynamic center (AC) plus a constant pitching moment M_0, also called M_{ac} or $M_{0.25c}$ since the AC is normally located at about 0.25 of the airfoil's chord (measured from the leading edge) [11]. However, for simulation purposes, Lift was applied to the structure along the caps of the main spar, which were located at $0.28\cdot chord_{local}$. Therefore, the associated wing pitching moment ($M_{0.28c}$) also had to be determined.

Wing Pitching Moment

Taking into consideration the linear twist and taper of the wing, the pitching moment distribution along the wing span (z direction) was obtained:

$$M_{0.28\cdot c_{half\_wing}}(z) = -\frac{1}{2}\cdot\left[\frac{2\cdot L_{wing}}{b\cdot(1+\lambda)}\cdot\left[1-\frac{2\cdot z}{b}\cdot(1-\lambda)\right]+\frac{4\cdot L_{wing}}{\pi\cdot b}\sqrt{1-\left(\frac{2\cdot z}{b}\right)^2}\right]\cdot\cos\left(\alpha_{twist}\cdot\left(1-\frac{2}{b}\cdot z\right)+\alpha_{tip}\right)\cdot\left[d_{root}\cdot\left[1-\frac{2\cdot z}{b}\cdot\left(1-\frac{d_{tip}}{d_{root}}\right)\right]+0.03\cdot c_{root}\cdot\left[1-\frac{2\cdot z}{b}\cdot\left(1-\frac{c_{tip}}{c_{root}}\right)\right]\right], \text{ with } 0\le z\le b/2 \quad (5)$$

Where α_{twist} is the wing's twist angle at the root, α_{tip} is the angle of attack at the tip of the wing, d_{root} and

d_{tip} are the distance between CP and AC measured along the airfoil's chord at the root and at the tip of the wing, respectively, c_{root} and c_{tip} are the chord of the airfoil at the root and at the tip of the wing, respectively.

The total pitching moment value was obtained from the integration of (5).

Weight and Inertial Forces

Wing Structure

Because, for the critical flight condition (Figure 5), the weight and the inertial force had coincident force vectors, a *total body force* (BF) was used instead:

$$W_{wing\_structure} = g \cdot m_{wing\_structure} \quad (6)$$

$$F_{inertial_{wing\_structure}} = (n-1) \cdot g \cdot m_{wing\_structure} \quad (7)$$

$$BF_{half-wing} = \mathrm{n}_{design} \cdot \frac{W_{wing\_structure}}{2} \quad (8)$$

The wing's initial mass was established to be the UAVision's estimated value of 26.2 [kg] since one of the objectives of this work was to lower the structural weight of the conceptual design, thus making this a conservative assumption.

Assuming that the wing, which had a trapezoidal geometry and constant taper and twist, also had an initial structure where components had constant thickness and were equally spaced along the wing span, the following body force (BF) distribution was obtained:

$$BF_{half-wing} \approx \frac{n \cdot 2 \cdot W_{wing}}{b \cdot (1+\lambda)} \cdot \left[1 - \frac{2 \cdot z}{b} \cdot (1-\lambda)\right], \textit{ with } 0 \le z \le b/2 \quad (8)$$

Additional Masses

Additional masses were attached to the wing structure and consisted of: a suspended payload pod and the two servo motors needed to actuate the ailerons and flaps (one for each). Their masses were 10, 0.2 and 0.2 [kg], respectively. The payload mass was imposed by operational requirements. The servo motors' mass was estimated based on the size of the wing and the force required to actuate its aerodynamic surfaces. From statistical data, servos with a force of 5 [kg/mm] have a mass $<$ 0.2 [kg]. The motors' mass approximation was therefore conservative.

These masses translated into weight and inertial force and, because the application points and force vectors were coincident (for each body), the resulting body forces were given by:

$$BF_{payload} = \mathrm{n}_{design} \cdot W_{payload} \quad (9)$$

$$BF_{motor\_1} = \mathrm{n}_{design} \cdot W_{motor\_1} \quad (10)$$

$$BF_{motor\_2} = \mathrm{n}_{design} \cdot W_{motor\_2} \quad (11)$$

2.3. Wing Structural Design

Before any structural design, it is a good practice to define which materials may be used because materials influence the design and the design influences how and what materials can be used.

2.3.1. Materials Selection

Nowadays, aircraft designers have a variety of high performance materials to choose from. Wanting to minimize the weight of the structure while still being able to maintain a high structural strength and stiffness, the materials chosen were carbon fiber laminate composites since they are the type of material with the best structural efficiency (best strength-to-weight ratio $\sigma_u/(\rho \cdot g)$ and best stiffness-to-weight ratio $E/(\rho \cdot g)$) [11]. Furthermore, knowing that the aircraft is expected to operate in a high salinity environment (maritime surveillance), the use of composite materials is also ideal due to their non-metallic nature which translates into the avoidance of corrosion problems.

As mentioned before, one of the limitations this work was to use the materials available at the FAP. From the materials available, the following were selected to be used in the structure:

- Bidirectional Carbon Fiber, 3K, High Strength (HS), 160 $[gr/m^2]$, P (plain weave);
- Unidirectional Carbon Fiber, 3K, HS, 215 $[gr/m^2]$, 15 [cm] tape;
- Epoxy Resin: SR 1500 + Hardener: Sicomin SD 2505 (100 [g] Epoxy - 33 [g] Hardener);
- Airex C70.75, thickness 3 [mm], (isotropic material);
- Kevlar 49, 195 denier, bidirectional, plain weave.

Many combinations of laminate composite materials could have been obtained from the materials selected, each one, with unique mechanical properties. In order to simplify the design process, and create a starting point for future material optimization studies, all the laminates created had all their plies oriented in the same direction (0º). Also, the percentages of resin and hardener as well as the curing conditions were kept the same for all materials: 100 [g] Epoxy - 33 [g] Hardener, 20ºC Cure, dry heat air conditioning, -0.5 [bar] vacuum, 24H duration.

Furthermore, in order to obtain a perception of how the physical characteristics of a composite change with the number of plies (thickness), different configurations were created. This was a crucial step because it allowed to understand the limitations of the materials in terms of their minimal thickness possible and associated porosity and permeability. These notions were essential for the translation of the theoretical project into a feasible one.

According to the information provided above, the following composite materials were manufactured using the hand-lay-up method:

- Epoxy + Bi Carbon Fiber (Bi CF): $[C_1^{0º}]$; $[C_2^{0º}]$; $[C_4^{0º}]$; $[C_{10}^{0º}]$; $[C_{11}^{0º}]$; $[C_{12}^{0º}]$; $[C_{13}^{0º}]$; $[C_{14}^{0º}]$;
- Epoxy + Uni Carbon Fiber (Uni CF): $[C_1^{0º}]$; $[C_2^{0º}]$; $[C_9^{0º}]$; $[C_{10}^{0º}]$; $[C_{11}^{0º}]$; $[C_{12}^{0º}]$;
- Epoxy + Bi Carbon Fiber + Airex: $[C_1^{0º}/A_1/C_1^{0º}]$;
- Epoxy + Airex: $[A_1]$;
- Epoxy + Kevlar: $[K_2^{0º}]$;
- Epoxy + Bi Carbon Fiber + Kevlar: $[C_1^{0º}/K_2^{0º}/C_1^{0º}]$;

Their relevant properties, for structural analysis purposes, were determined using experimental procedures, conducted in accordance with regulations from the American Society for Testing Materials (ASTM). All the necessary properties that could not be obtained via experimental means were obtained from statistical data [15] or, as a last resort, using theoretical methods (*rule of mixtures* for the unidirectional carbon fiber composites and, formulas from [16], for the bidirectional composites). For the foam, the properties that could not be obtained via experimental means were obtained from the manufacturer [17]. The cost of each material was also determined.

All the experimentally obtained values were found to be in accordance with theoretical and statistical data.

2.3.2. Initial Design

An initial wing structure was idealized in order to meet all the aircraft's structural and operational requirements.

Because Flaps and Ailerons have a minimal contribution to the wing's overall capability to withstand maximum loads, they were considered not to be part of the wing structure. Their individual structures would be addressed later on. The non-inclusion of these trailing edge devices was a conservative approximation because their inclusion would further, slightly, increase the wing structural rigidity and decrease the maximum stresses. Although this devices were not part of the designed structure, their forces and moments were still present and applied to the wing structure since they influence the forces determined in section 2.2.2.

For the half-wing without the aileron or the flap, the components that made up the structure, as well as their respective locations, were defined as follows:

- **Skin:** Plain geometry; Constant thickness throughout the span;
- **1st Spar:** Located at where the airfoil is thickest (in this case $0.28 \cdot c(z)$) in order to maximize the Spar's *area moment of inertia* (I) and consequently maximize its effectiveness to resist bending loads; Along the full length of the wing plus a root extension for attachment purposes (wing to fuselage); Constant thickness; Constituted by 2 Caps and 5 Webs: Caps in permanent contact with the skin; Webs kept in a vertical position throughout the span and unequally spaced: 1 at the middle, 1 at 1/3 and 1 at 2/3 of the Caps' width;
- **2nd Spar:** Located near to the hinge axis of the trailing edge devices (flap and aileron); Along the full length of the wing plus a root extension for attachment purposes (wing to fuselage); Constant thickness; Constituted by 2 Caps and 2 Webs arranged in a "box" configuration (quadrangular cross-section): Caps in permanent contact with the skin; Webs kept in a vertical position throughout the span.
- **9 Ribs:** Plain geometry; All with the same thickness; Placed at the following locations: Wing root; Wing tip; Payload location; Motor 1 attachment area inner border and outer border; Motor 2 attachment area inner border and outer border; and another two Ribs to close skin gaps.

Additional design features:

Holes: Holes were made on the skin and ribs. A "laminate drilling damage factor for bidirectional composites" of $\frac{5}{3}$ was established and used thus, the holes were designed as having a diameter equal to the damage (delamination) diameter instead of their true diameter.

<u>Ribs</u>:

- 2 holes per Rib were drilled in order to allow for the passage of electrical wires, also being useful for water drainage or internal structural inspection.

<u>Skin</u>:

- 12 holes were drilled in the payload attachment area to allow for the bolted connection; 8 holes were drilled in each of the servo motors attachment areas to allow for bolted connections;

Cut-outs: "Cut-outs" can be created by either cutting away material or by not adding material to that area during a component's construction (in the case of composite laminate materials).

<u>Skin</u>:

- Two cut-outs were created in the center of both servo motors attachment areas (on the Skin). These were dimensioned to be large enough to allow for the servo motor to pass through the opening and to be installed inside the wing. Due to the quadrangular geometry of the cut-outs, their vertices were rounded in order to minimize maximum stresses on the edges of the openings. The best corner radius was determined from [18].

Attachment Areas: In order to comply with regulation's specifications, the attachment areas of both the payload and the servo motors were dimensioned so that the distance from their border to any hole border would always be larger than the hole true diameter.

From the parameters defined above, the *wing structure initial model* was represented by modeling its components as 2D shells, Figure 6:

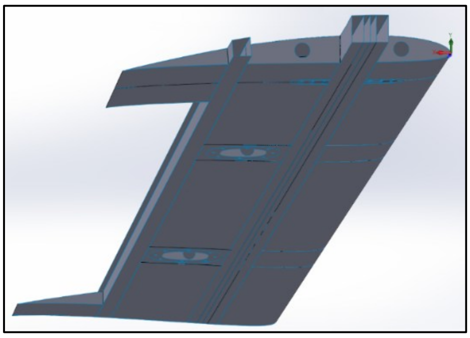

a)

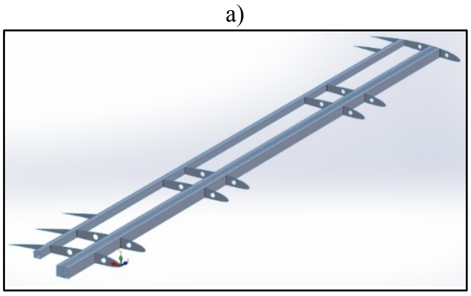

b)

Figure 6 - Wing structure initial model: a) Bottom view of the external surface (skin) with holes and cut-outs for the payload and servo motors; b) Wing internal structure: two Spars and nine Ribs.

2.4. Wing Structural Analysis and Optimization

For purposes of structural analysis, it was decided to use a finite element analysis (FEA). In order to save computation time, the *wing structure initial model* was simplified. This simplification also served the purpose of creating an initial structure as simple as possible for the purpose of establishing a starting point for the subsequent step-by-step logical optimization of each structural component.

For both the FEA and the modelation of the various geometric configurations, the software SolidWorks 2016 (SW) was used.

2.4.1. Geometric Model Simplification

The simplifications performed were the following: suppression of holes and cut-outs in the skin, suppression of holes and cut outs in the ribs, suppression of the root extensions. See Figure 7.

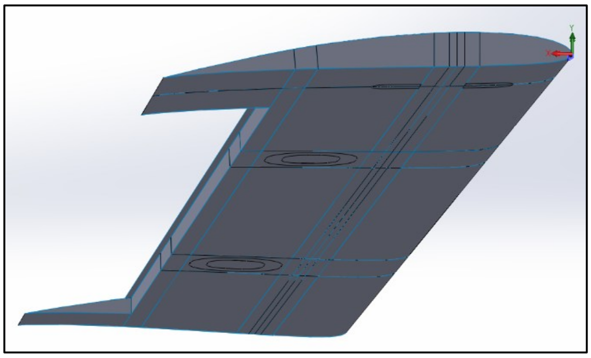

Figure 7 - Simplified Initial Model.

Another simplification which greatly contributed to the reduction of the simulation time was to maintain the model designed as 2D shells instead of 3D which is an approximation that can be performed for structures which components are made up of thin sheets of material (as was this case). This approximation was found to be conservative in terms of the maximum stress value.

2.4.2. Material Atribution

In order for the *Simplified Initial Model* to become the starting point for the optimization process, a single material and a single thickness were attributed to all the 2D shells that made up the structure (Epoxy + Bi CF $[C_{10}^{0^{\circ}}]$ and thickness of 1.9 [mm]), see Figure 8.

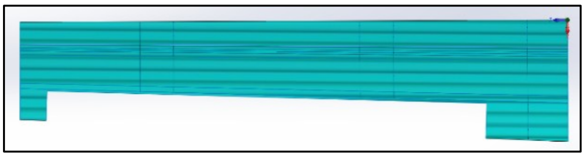

a)

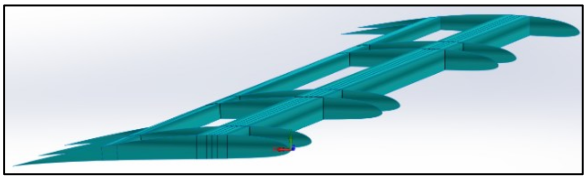

b)

Figure 8 - Material 0º Direction: a) Simplified model: Skin and Caps; b) Simplified model: Ribs and Webs.

Regarding the thickness, most 2D shells (surfaces) did not have their thickness symmetrically attributed since those were not "mid-plane" surfaces but rather "top" or "bottom" surfaces.

2.4.3. Mesh Definition and Mapping

All the surfaces were discretized in FE of the type "triangular" with a "standard mesh" and the option "Draft Quality Mesh" was selected. Also an initial value for the "Global FE size" and "Tolerance" were selected, see Figure 9.

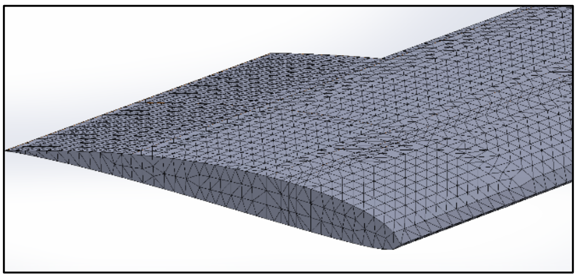

a)

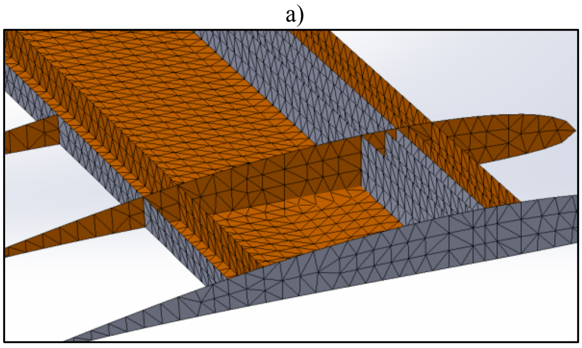

b)

Figure 9 - Various components' meshes and respective nodes coincidence: a) Detail: coincidence between Skin and Rib nodes; b) Detail: coincidence of multiple nodes belonging to: Skin, Spars, Ribs, payload attachment area.

After meshes had all been attributed, they were checked using the command "Render shell thickness in 3D", allowing to check the mesh quality and also, if the thicknesses that been properly attributed, see Figure 10.

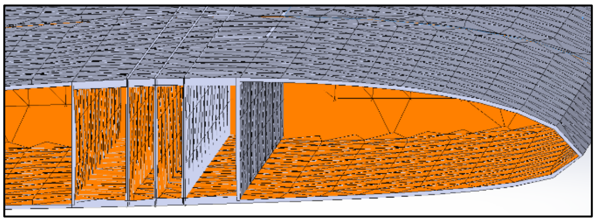

Figure 10 – Components thicknesses.

2.4.4. Boundary Conditions

The structure was placed under a cantilever boundary condition as follows (see Figure 11):

- The root edges of the both Spars were "fixed"- no rotation and no displacement - in order to simulate the wing attachment to the fuselage (usually to a bulkhead mounted on the interior of the fuselage);
- The outer surface of the Rib at the root ($z = 0$) was put under a "roller-slider" condition in order to simulate the sliding contact between the Rib at the root and the fuselage skin.

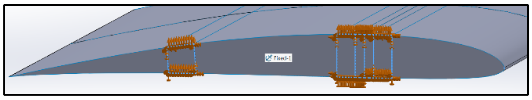

a)

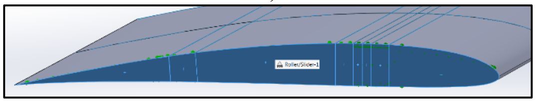

b)

Figure 11 – Cantilever boundary condition.

2.4.5. Forces and Moments

The force $F_{root-cantilever}$ was applied to the structure via the cantilever boundary condition applied to the root of the wing. The aerodynamic loads, pitching moment, inertial loads and weight, were applied to the structure as follows (see Figure 12):

- The Lift distribution function was applied on both caps of the 1st Spar in the positive y direction;
- The Pitching Moment distribution function was applied on both caps of the 1st Spar, using the 1st Spar axis as the reference torsional axis.
- The Payload Body Force was applied to its delimited "attachment area" on the skin in the negative y direction.
- The Motor_1 and Motor_2 Body Forces were applied to their delimited "attachment area" on the skin in the negative y direction.
- Because the SW allows to apply an acceleration to a structure under analysis, the previously determined wing structure's Body Force was replaced by an acceleration in the negative y direction given by:

$$a_y = n_{design} \cdot g \cdot \cos(\alpha) \cdot \cos(\Gamma) \tag{9}$$

Where α is the wing's angle of attack and Γ is the wing's dihedral angle.

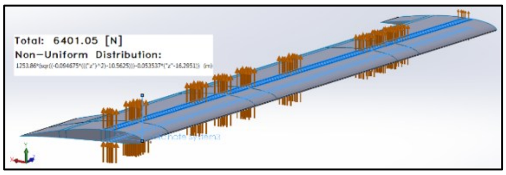

a)

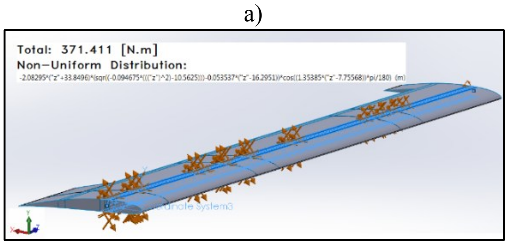

b)

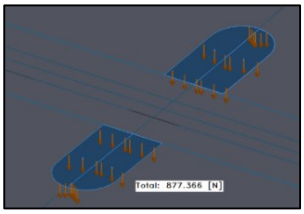

c)

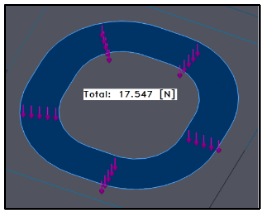

d)

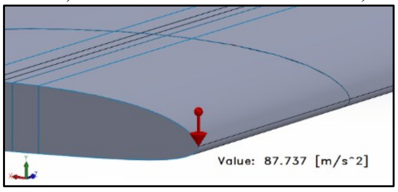

e)

Figure 12 - Forces and Moments applied on the structure: a) Lift; b) Pitching Moment; c) Payload Body Forces; d) Motor 1 or 2 Body Forces; e) Structure's Acceleration.

2.4.6. Analysis (FEA)

A structural analysis of the type "Static" was performed and the outputs "Von Mises Stress" and "Displacement" were selected. From these, the maximum stress and maximum displacement were recorded.

The next step consisted in the convergence analysis of the finite elements (FE) size, resulting in the selection of a value that allowed for good meshing and acceptable computational times while ensuring the existence of convergence in the simulation outputs.

Applying the new FE size and tolerance a new simulation was run for the *Simplified Initial Model* and the values of maximum Von-Mises stress and Displacement were recorded. See Figure 13.

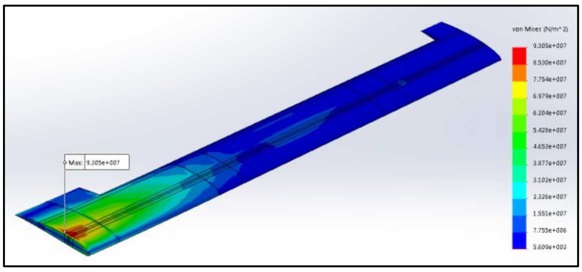

a)

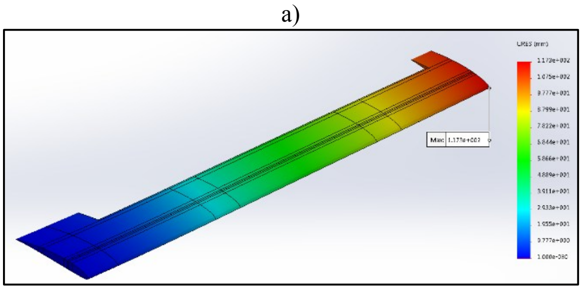

b)

Figure 13 – a) Von Mises Stresses across all plies with maximum Stress localized at the wing root; b) Wing Displacement with maximum Displacement localized at the wing tip.

At this point, the mass of the structure was also estimated / calculated in a conservative manner, based on the total surface area, the attributed thicknesses and the material density.

Comparing the obtained values with the structural and mass requirements set for the wing, it was concluded that the *Simplified Initial Model* satisfied all the structural requirements in terms of strength and rigidity however, in terms of weight, knowing that the UAVision's estimation for the half-wing total weight also included the flap and the aileron, the final weight of the present half-wing model would be higher than the target value. Therefore, in order to significantly reduce the mass of the structure while guaranteeing the fulfillment of the structural requirements, an optimization process was undertaken.

2.4.7. Structural Optimization

A "chain top-down" approach was created and used in order to optimize the structure by individually optimizing each component in the following order (from first to last): Skin, 1st Spar, 2nd Spar, Ribs. This chain top-down approach could be described as a "hierarchic decomposition method" and it was inspired by the logic behind the "topological optimization method" - which uses stress lines as the guides for the shape optimization of a given material volume. The optimization process consisted of four main steps:

Step 1:

- Definition of the best cross-section geometric configuration for each component, which minimized the structure's maximum stress (σ_{max}).
  Restrictions:
  - Components' locations maintained;
  - Components with constant thickness throughout the span;
  - Components' mass kept constant.

Step 2:

- Definition of each component's mass relevance for the minimization of the σ_{max}.

Step 3:

- Redistribution and minimization of the total mass of the structure. Restrictions:
  - Fulfillment of the structural requirements;
  - Feasibility of manufacturing – one of the factors being the material's minimum possible thickness.

Step 4:

- Reintroduction of the Skin holes and cut-outs and dimensioning of their reinforcements;
- Study of the possibility of replacing materials in order to further reduce the structure's total mass;
- Reintroduction of the root extension.

At the end of Step 4 a successfully optimized structure was obtained. Figure 14 shows the FEA analysis results for that *Final Geometric Configuration.*

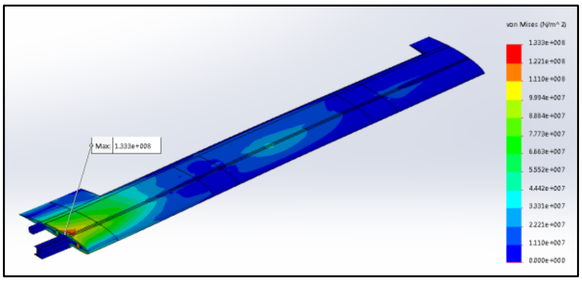

a)

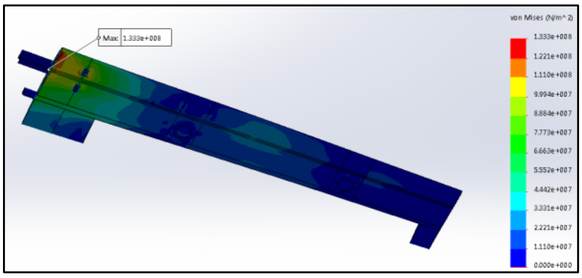

b)

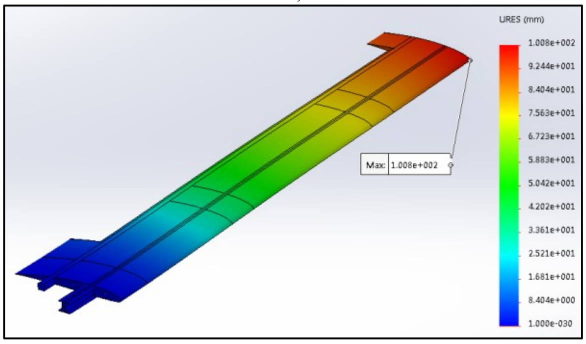

c)

Figure 14 - a) and b) Von Mises Stresses across all plies with maximum Stress localized at the wing root; c) Wing Displacement with maximum Displacement localized at the wing tip.

2.5. Wing Final Design including Flaps and Ailerons

The wing structure final design corresponded to the *final geometric configuration* resultant from the optimization process. Nevertheless, there was the need to obtain a *Complete Wing Geometric Configuration*, which included the Flaps and the Ailerons, in order to properly estimate the full weight of the wing, thus allowing to assess if it already complied with the weight requirement (< 26.2 [kg]), and to estimate the final construction cost of the complete wing.

2.5.1. Complete Wing and Weight and Cost Estimation

In order to obtain a complete wing geometric configuration, the Flaps and Ailerons structures were defined based on the premise that they could be considered "scaled down wings" therefore, their structures were defined as being constituted by: Skin, one Spar and three Ribs, although no structural study was performed for none of them.

The Flaps and Ailerons component's design, thickness and positioning were proposed based on their predictable manufacturing process resulting in the following:

- Ribs: same thickness and lamination as the Ribs of the main structure; one placed at the mid-span and one at each end;
- Spar: with the same shape and lamination configuration as the 2nd Spar; placed at the Flap or Aileron "leading-edge";
- Skin: Same thickness and lamination as the Skin of the main structure.

The hinged connection between the ailerons and flaps and the main wing structure was designed to be made out of two plies of Kevlar 49.

For the assembly of the whole wing, a quantity of Epoxy, equivalent to a ply with a thickness of 0.1 [mm], was estimated (based on the manufacture experience gained from the production of the material's specimens) to be necessary in order to connect the various components.

Adding up the mass contributions of all the wing's components (Skin, Spars and Ribs) and connection agents (Epoxy 0.1 [mm] "ply"), not one but three possible final mass values were obtained for the wing. Those depended on the type of resin impregnation method chosen to be used during the manufacturing process of the Skin - sandwich composite laminate with foam core - which would directly affect the amount of resin "trapped" in the foam (Airex C70.75) porous surface.

For each one of those three methods – use of "store bought" Prepreg, Pre-impregnation by hand-lay-up and No Pre-impregnation - three different manufacturing costs (based solely on material costs) were determined.

2.5.2. Wing Final Design, Characteristics Summary

The final wing structure satisfied all structural, mass and operational requirements imposed:

- Capable of enduring: 4 and -1.5 G's;
- $\sigma_{max} = 133.3\ [MPa]$ < 570.0 [MPa] - Ultimate (and yield) compressive strength in x (0º) of the material Epoxy + Bi CF [$C_{10}^{0º}$];
- $\sigma_{\max\_foam\ plies} \approx 1$ < 1.45 [MPa] – Airex C70.75 compressive strength. Also, $\sigma_{\text{average}\_foam\ plies} \approx$ 0.15 [MPa];
- $d_{max} = 100.8\ [mm]$ < 162.5 [mm] - Structural stiffness requirement stated that the wing tip displacement should be inferior to 5% of the wing's half span (3250 [mm]);
- $mass_{wing}$ = 18.07 / 21.464 / 24.86 < 26.2 [kg] - UAVision's weight estimation for the full wing.
- Each half-wing capable of carrying up to 10 [kg] of suspended payload;
- Materials used (composite materials) capable of enduring high salinity environments without suffering corrosion problems;
- Long service life expected due to the large margin between the working stress and the maximum (design) stress.

How much the initial predicted mass of 26.2 [kg] was reduced, depended on the impregnation method used on the Skin: 31% (Prepreg); 18% (Pre-impregnation by hand-lay-up) or 5% (Hand-lay-up).

The lowest manufacturing cost, based solely on material costs, corresponded to the Pre-impregnation: 2x 1107.12€, followed by the Hand-lay-up: 2x 1315.70€, and the highest, to the use of Prepregs: 2x 1451.68€. Despite the higher manufacturing cost, the use of Prepregs on the Skin would be ideal since it significantly reduced the total mass of the wing, in comparison to any other methods, therefore significantly reducing operational costs and increasing the aircraft's operational capabilities.

All the materials needed for the manufacturing of the wing would be:

- Bidirectional Carbon Fiber, 3K, HS, 160 $[gr/m^2]$, (plain weave) ("normal" hand-lay-up impregnation) ($C_n^{nº}$). Quantity: ≈ 32.32 $[m^2]$ (if no Pre-impregnation or Prepreg is used); ≈ 23.77 $[m^2]$ (if Pre-impregnation or Prepreg is used);
- Bidirectional Carbon Fiber Pre-impregnated or Equivalent Prepreg material ($Cp_n^{nº}$). Quantity: 8.55 $[m^2]$;
- Epoxy Resin: SR 1500 + Hardener: Sicomin SD 2505 (100 [g] Epoxy - 33 [g] Hardener). Quantity: ≈ 2.750 [kg] (if Prepreg is used); ≈ 5.740 [kg] (if no Pre-impregnation is used); ≈ 7.776 [kg] (if normal hand-lay-up method is used);
- Airex C70.75, thickness 3 [mm], (isotropic material) (A_n). Quantity: ≈ 3.40 $[m^2]$;
- Kevlar 49, 195 denier, bidirectional, plain weave ($K_n^{nº}$). Quantity: ≈ 0.177 $[m^2]$.

From these materials the configurations created for each component would be the following:

Skin:

- Areas over the spars' caps: $[C_2^{0º}]$ or $[Cp_2^{0º}]$ – 0.38 [mm];
- "Attachment areas" of the servo motors: $[C_{18}^{0º}]$ or $[Cp_1^{0º}/C_{16}^{0º}/Cp_1^{0º}]$ – 3.42 [mm];
- Kevlar hinged connection: $[C_1^{0º}/K_2^{0º}/C_1^{0º}]$ or $[Cp_1^{0º}/K_2^{0º}/Cp_1^{0º}]$ – 0.64 [mm] and $[C_1^{0º}/K_1^{0º}/A_1/K_1^{0º}/C_1^{0º}]$ *or* $[Cp_1^{0º}/K_1^{0º}/A_1/K_1^{0º}/Cp_1^{0º}]$ – 3.64 [mm];
- All other skin areas: $[C_1^{0º}/A_1/C_1^{0º}]$ *or* $[Cp_1^{0º}/A_1/Cp_1^{0º}]$ – 3.38 [mm].

1st Spar:

- Caps: $[C_{27}^{0º}]$ – 5.13 [mm]; Webs: $[C_8^{0º}]$ – 1.52 [mm].

2nd Spar:

- Caps: $[C_8^{0º}]$ – 1.52 [mm]; Webs: $[C_7^{0º}]$ – 1.33 [mm].

Ribs:

- $[C_8^{0º}]$ – 1.52 [mm].

For all components, except the Ribs and the Kevlar hinges, the 0º orientation of the material's fibers is coincident with the direction of the 1st Spar axis ($\neq z$). For the Ribs, the 0º orientation is coincident with the x axis. For the Kevlar hinge, the 0º orientation is coincident with the direction perpendicular to the 2nd Spar axis.

The curing process needed to ensure the mechanical characteristics of the structure was the following: vacuum bag at -0.5 [bar] during 24H, at a room temperature of 20ºC, with the air-condition system set to dry heat (low humidity environment).

2.5.3. 3D Solid Designs and Detailed Mapping of Materials

In order to better visualize the final design of the wing and to better understand how and where each material should applied, the wing was modeled as a 3D solid, see Figure 15.

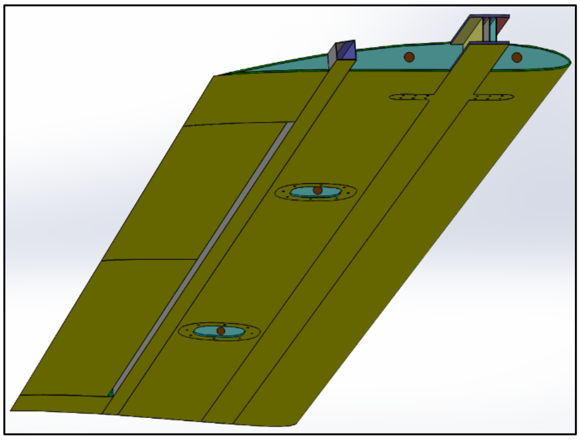

a)

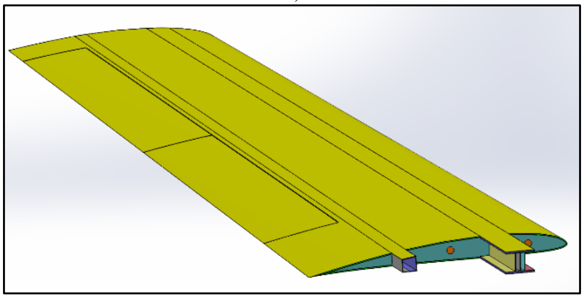

b)

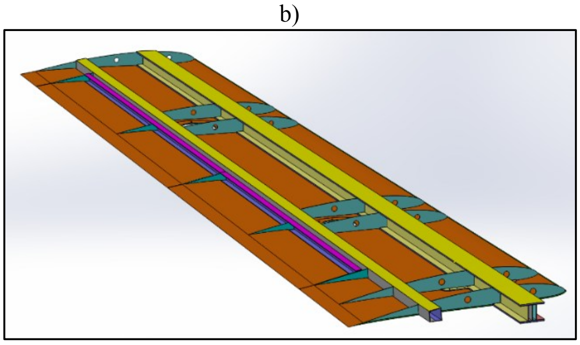

c)

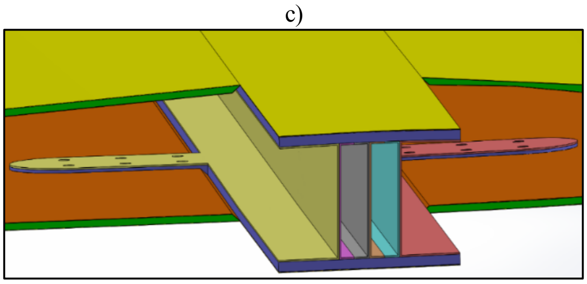

d)

Figure 15 – a) and b) Complete Wing Geometry; a) Bottom view; b) Top view; c) Bottom Skin of the main structure + 1st Spar + 2nd Spar + Flap Spar + Aileron Spar + all Ribs; d) Detail: 1st Spar root.

The 3D solid model was designed in a dimensionally accurate manner so that it could be used as a guide for manufacturing purposes and / or as the basis for future detailed designs.

3. Conclusions

The design and optimization of the wing structure was a challenging project which required a proactive and iterative approach to the design by balancing three fundamental criteria:

- Design;
- Materials selection;
- Manufacturing processes.

It involved:

- Determining the loads on the structure;
- Planning the general shape and layout;
- Choosing materials;
- Shaping, sizing and optimizing its many components.

With the objectives of:

- Fulfilling structural, operational and certification requirements;
- Minimizing manufacturing costs;

The resulting wing structure, which included flaps and ailerons, complied with all requirements and was estimated to have a manufacturing cost, in terms of materials, close to 3000 €.

References

[1] "Portuguese Airspace Under Portugal Responsibility," [Online]. Available: https://www.nav.pt/en/nav/air-navigation-services-1/airspace. [Accessed 2016].

[2] "SRR (Search and Rescue Region)," Esquadra 751, 2016. [Online]. Available: http://www.emfa.pt/www/po/esquadra/link-751-013.006.001-descricao.

[3] "A Marinha ao Serviço de Portugal," Marinha Portuguesa, 2016. [Online]. Available: http://www.marinhasplp.org/PT/asmarinhas/doutrinas/Documents/A%20Marinha%20ao%20Servi%C3%A7o%20de%20Portugal_23MAR.pdf.

[4] "A Vigilância Marítima na Força Aérea," Força Aérea Portuguesa, 2016. [Online]. Available: http://www.emfa.pt/www/noticia-480-a-vigilancia-maritima-na-forca-aerea.

[5] "Busca e Salvamento Marítimo," Marinha Portuguesa, 2016. [Online]. Available: http://www.marinha.pt/pt-pt/marinha/busca-e-salvamento/Paginas/default.aspx.

[6] "Portugal, uma nação marítima," Marinha Portuguesa, 2016. [Online]. Available: http://www.marinhasplp.org/PT/asmarinhas/doutrinas/Documents/Portugal_uma_nacao_maritima.pdf.

[7] G. Oduntan, "Sovereignty and Jurisdiction in Airspace and Outer Space: Legal Criteria for Spatial Delimitation," 2011. [Online]. Available: http://landingbook.co/sovereignty_and_jurisdiction_in_airspace_and_outer_space_legal_crit

eria_for_spatial_delimitation_routledge_research.pdf.

[8] "SAR," Esquadra 502, 2016. [Online]. Available: http://www.emfa.pt/www/po/esquadra/link-502-005.002.003.003-sar.

[9] UAVision, *MALE Prototype, Preliminary Specs,* UAVsision.

[10] "Airfoil S4110," Airfoil Tools, 2016. [Online]. Available: http://airfoiltools.com/airfoil/details?airfoil=s4110-il.

[11] S. A. Brandt, R. J. Stiles, J. J. Bertin and R. Withford, "Introduction to Aeronautics: A Design Perspective," Second Edition ed., AIAA Educational Series, 2004, pp. 74-75; 85; 90; 145; 225; 228; 230; 302; 315; 319-320; 323; 325-326; 329-332; 335; 340.

[12] P. F. F. d. Albuquerque, *Structural Loads Handbook, Dissertação de Mestrado em Engenharia Aeroespacial,* Instituto Superior Técnico, 2011, pp. 3-8.

[13] *Certification Specification for Large Aeroplanes (CS-25) - Subpart C - Structure,* European Aviation Safety Agency, 2010.

[14] NATO, *Light Unmanned Aircraft Systems Airworthiness Requirements, NATO STANDARD AEP-83,* NATO Standardization Agency (NSA) NATO/OTAN, 2014.

[15] *Mechanical Properties of Carbon Fibre Composite Materials, Fibre / Epoxy resin (120ºC),* Performance Composites Ltd, 28/03/2017.

[16] D. Gay, S. V. Hoa and S. W. Tsai, *Composite materials design and applications,* London, New York, Washington: Boca Raton, 2003.

[17] AIREX and BALTEK, *Airex C70, Universal Structural Foam, DATA SHEET, 07.2011,* 3A Composites.

[18] S. R. Heller, "Stress Concentration Factors for a Rectangular Opening with Rounded Corners in a Biaxially Loaded Plate," *Journal of Ship Research,* September 1969.